

Green Chemistry

Accepted Manuscript



This article can be cited before page numbers have been issued, to do this please use: X. Li, K. Zhang, S. Chen, C. Li, F. Li, H. Xu and Y. Fu, *Green Chem.*, 2018, DOI: 10.1039/C7GC03072J.



This is an Accepted Manuscript, which has been through the Royal Society of Chemistry peer review process and has been accepted for publication.

Accepted Manuscripts are published online shortly after acceptance, before technical editing, formatting and proof reading. Using this free service, authors can make their results available to the community, in citable form, before we publish the edited article. We will replace this Accepted Manuscript with the edited and formatted Advance Article as soon as it is available.

You can find more information about Accepted Manuscripts in the [author guidelines](#).

Please note that technical editing may introduce minor changes to the text and/or graphics, which may alter content. The journal's standard [Terms & Conditions](#) and the ethical guidelines, outlined in our [author and reviewer resource centre](#), still apply. In no event shall the Royal Society of Chemistry be held responsible for any errors or omissions in this Accepted Manuscript or any consequences arising from the use of any information it contains.



Journal Name

ARTICLE

Cobalt catalyst for reductive etherification of 5-hydroxymethylfurfural to 2,5-bis(methoxymethyl)furan under mild conditions

Xing-Long Li,^a Kun Zhang,^{a,b} Shi-Yan Chen,^{a,b} Chuang Li,^a Feng Li,^a Hua-Jian Xu,^{*c} and Yao Fu^{*a}

Received 00th January 20xx,
Accepted 00th January 20xx

DOI: 10.1039/x0xx00000x

www.rsc.org/

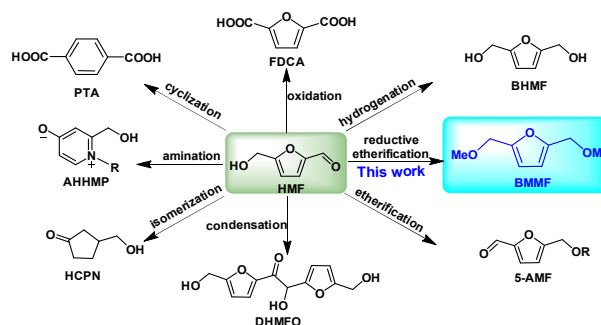
Conversion of platform molecule 5-hydroxymethylfurfural (HMF) into high-value-added derivatives has attracted significant interest. In this paper, metallic cobalt catalyst was prepared by simple reduction of commercially available Co_3O_4 , and used to catalyze the reductive etherification of HMF to 2,5-bis(methoxymethyl)furan (BMMF) under mild conditions. A yield of 93% 2,5-bis(hydroxymethyl)furan (BHMF) was obtained (90 °C, 2 MPa H_2 , 1 h) and 98.5% yield of BMMF was achieved (140 °C, 2 MPa H_2 , 1 h) by using Co-400 catalyst. The catalysts were characterized by X-ray photoelectron spectroscopy (XPS), powder X-ray diffraction (XRD), and ammonia-temperature-programmed-desorption (NH_3 -TPD), Scanning electron micrographs (SEM), Transmission Electron Microscopy (TEM) and Inductively Coupled Plasma Atomic Emission Spectroscopy (ICP-AES). It was found that the Co^0 and $\text{Co}^{2+/3+}$ species were coexisted on the surface of catalyst and the catalyst became more porous and rougher after reduction at high temperature. This may be more beneficial for enhancing the selectivity of etherification product and the mass transfer of reaction species. A possible reaction mechanism was proposed based on GC and $^1\text{H-NMR}$ analyses. The cobalt catalyst was reused five times with a slight decrease in activity.

Introduction

Severe resource crises and environmental problems have been created along with the depletion of fossil fuels. In this context, researchers have focused more attention on the conversion of renewable resources into valuable products. Given that biomass resources constitute the only renewable carbon source, it is of great significance to synthesize high-value-added fuels and chemicals from biomass resources.¹

5-Hydroxymethylfurfural (5-HMF), obtained from the hydrolysis of lignocellulose, is recognized as an important potential platform molecule that can be converted into a range of high-value-added chemicals through the application of etherification,² oxidation,³ hydrogenation,⁴ amination,⁵ isomerization,⁶ condensation,⁷ and cyclization reactions,⁸ etc. (Scheme 1).⁹ Furfuryl alkyl ethers and their derivatives are important chemical raw materials that can be used as pharmaceuticals, pesticides, spices, food additives, surfactants, fuel additives, paint remover, and rubber modifiers, etc.¹⁰ For instance, 2,5-bis(ethoxymethyl)furan (BEMF) has been assessed

as a diesel additive in a six-cylinder heavy duty engine and no significant difference in engine operation was found for any of the tested blending ratios.¹¹ 2-(Alkoxy)methylfuran,^{12a} 2-(alkoxy)methyltetrahydrofuran,^{12b} and bis(tetrahydrofurfuryl)-ether,^{12c} etc. are also potential biodiesel candidates.



Scheme 1. The conversion of HMF into high-value-added products through different reaction pathways.

Considering the multiple applications and high value of etherified products, it is of great interest to investigate the conversion of biomass platform molecules into furfuryl alkyl ether. To date, the etherification of HMF has mostly resulted in either the monoether derivative or dimers.¹³ Approaches used for the preparation of furfuryl alkyl ethers can be classified as follows. 1) Halogenation of furan alcohols followed by etherification with aliphatic alcohols; however, the use of equivalent halogenated agent was poor in terms of atom economy.^{14a} 2) The use of 5-chloromethylfurfural as an intermediate and $\text{Ar-SO}_3\text{H-SBA-15}$ as the

^a Hefei National Laboratory for Physical Sciences at the Microscale, iChEM, CAS Key Laboratory of Urban Pollutant Conversion, Anhui Province Key Laboratory of Biomass Clean Energy, Department of Chemistry, University of Science and Technology of China.

Hefei 230026, China. Fax: (+86) -551-63606689;

E-mail: fuyao@ustc.edu.cn

^b Nano Science and Technology Institute, University of Science and Technology of China, Suzhou 215123, P. R. China.

^c School of Biological and Medical Engineering, Hefei University of Technology, Hefei 230009, China. Fax: (+86) -551-62904405;

E-mail: hixu@hfut.edu.cn

Electronic Supplementary Information (ESI) available: [details of any supplementary information available should be included here]. See

catalyst to obtain EMF. The obtained ethyl levulinate, formed in the etherification reaction, was attributed to the presence of strong Brønsted acid.^{14b} 3) The most common method is the direct etherification of furan alcohols and monohydric alcohols in the presence of acid catalyst. For instance, acidic molecular sieve ZSM-5 (Si/Al=25) was used as catalyst to catalyze the etherification of furfuryl alcohol and ethanol. However, the selectivity of furfuryl ethyl ether was only 44.8%.^{12b}

The synthesis of 2, 5-bis (alkoxymethyl) furan required hydrogenation of HMF to BHMF first, followed by etherification mediated by acidic catalyst to obtain 2, 5-bis (alkoxymethyl) furan. The reductive etherification has been catalyzed by transition-metal catalysts,¹⁵ Lewis acids,¹⁶ Brønsted acids,¹⁷ and thiourea organocatalyst.¹⁸ To date, the reductive etherification of HMF has proceeded in low yield, mainly because of competing reactions such as the formation of levulinic acid, or the reductive homocoupling of the aldehyde component as well as the formation of humin.¹⁹ Balakrishnan *et al.* studied reductive etherification of HMF to 2, 5-bis (alkoxymethyl) furan by using a PtSn/Al₂O₃ and Amberlyst-15 co-catalyst system under hydrogen pressure in one pot.²⁰ They obtained the corresponding 2, 5-bis (alkoxymethyl) furan in yields of 64% and 47% by using ethanol and *n*-butanol, respectively. Gruter *et al.* investigated the continuous hydrogenation and etherification of HMF to 2, 5-bis (ethoxymethyl) furan. HMF was hydrogenated to 2, 5-bis (hydroxymethyl) furan (BHMF) over Pt/C catalyst first and then etherified to 2, 5-bis (ethoxymethyl) furan at 348 K without hydrogen.²¹ The yield of 2, 5-bis (ethoxymethyl) furan reached 75%. Mu *et al.* applied a two-step method to obtain 70% yield of BMMF from HMF by using a Cu/SiO₂ and HZSM-5 co-catalyst system.²² Solid acid catalysts, such as Sn-Beta and Zr-Beta, were used for the reductive etherification of HMF to BMMF through the Meerwein–Ponndorf–Verley reaction (MPV reaction). The authors found that appropriate substrate concentration and sufficient numbers of acid–base sites were both important to obtain high yields of the etherified products.²³ Nowadays, the conversion of HMF into BMMF is generally realized by using a catalyst system containing hydrogenation catalyst and acid catalyst. However, it remains challenging to obtain high yields of reductive etherification products under mild conditions using a bifunctional catalyst containing both hydrogenation activity and etherification activity.

Cobalt-based catalysts have many important applications, and they can catalyze oxidation, hydrogenation, and isomerization reactions, *etc.* under mild conditions. Cobalt-based catalysts retain both hydrogenation activity and Lewis acid acidity even after reduction due to the coexistence of Co⁰ and Co^{2+/3+} species.²⁴ Indeed, in our previous work, we also found that the reduced cobalt-based catalyst contains both Co⁰ and Co^{2+/3+} species.²⁵

In this work, we wanted to develop an effective approach to convert 5-HMF into BMMF by using a Co catalyst. The Co catalyst was obtained by simple reduction of commercially available Co₃O₄. Parameters such as reaction temperature, reaction time, reaction pressure, and substrate concentration, *etc.* were investigated in detail. ¹H-NMR analysis and reaction dynamic studies were also conducted to help clarify the reaction mechanism, and a possible reaction pathway is proposed. The recycling and reuse of the Co catalyst are also discussed. The preparation of BMMF from fructose in two-steps is also studied.

Experimental Section

Materials and reagents

Co₃O₄, Fe₃O₄, CuO, Raney Ni, methanol (AR), N,N-dimethylformamide (AR), hydrochloric acid (AR), sulfuric acid (AR), sodium hydroxide (AR), sodium bicarbonate (AR), sodium borohydride (AR), dichloromethane (AR), isopropyl alcohol (AR) were purchased from Sinopharm Chemical Reagent Co. Ltd. 5-hydroxymethylfurfural was supplied by Hefei Leaf Biotech Co., Ltd (www.leafresource.com). Pure water was purchased from Wahaha, Hangzhou. The preparation methods of the possible intermediates and products were listed in Supporting Information.

Catalyst preparation and characterization

Co₃O₄ was reduced by increasing the temperature from 30 °C to 400 °C and the gas composition was H₂: N₂ (10:90, 100 mL/min), at the rate of 2 °C/min. After holding for 2 h at 400 °C, turned off the hydrogen and dropped to room temperature under nitrogen, then took out the catalyst, bottled it and marked as Co-400 catalyst. Other Co catalysts with different reduction temperature were reduced and labelled with similar methods. Fe₃O₄ was reduced at atmospheric pressure by increasing the temperature from 30 °C to 500 °C and the gas composition was H₂: N₂ (10:90, 100 mL/min), at the rate of 2 °C/min. After holding for 2 h at 500 °C, turned off the hydrogen and dropped to room temperature under nitrogen, then took out the catalyst and bottled it. CuO was reduced at atmospheric pressure by increasing the temperature from 30 °C to 240 °C and the gas composition was H₂: N₂ (10: 90, 100 mL/min), at the rate of 2 °C /min. After holding for 2 h at 240 °C, turned off the hydrogen and dropped to room temperature under nitrogen condition, then took out the catalyst and bottled it.

Catalysts were characterized by X-ray photoelectron spectroscopy (XPS), X-ray diffraction (XRD), Ammonia-Temperature-Programmed-Desorption (NH₃-TPD), Scanning electron micrographs (SEM), Transmission Electron Microscopy (TEM) and Inductively Coupled Plasma Atomic Emission Spectroscopy (ICP-AES). X-ray power diffraction (XRD) patterns of catalysts were obtained on X'pert (PANalytical) diffractometer with Ni-filtered Cu-K α radiation, at 40 kV and 40 mA. 2 θ range was 20°~80°. X-ray photoelectron spectra (XPS) data were obtained with a Thermo Scientific Escalab 250-X-ray photoelectron spectrometer which equipped a hemispherical electron analyzer and an Al K α X-ray source. All binding energies were referenced to C1s line at 284.7eV. Ammonia-Temperature-Programmed-Desorption (NH₃-TPD) tests: the catalysts were treated at 500 °C under helium flow (ultrahigh purity, 20 mL·min⁻¹) for 2 h, and the adsorption of ammonia was carried out at 40 °C for 1 h. After that, the catalysts were flushed with helium at 40 °C for 1 h, and the programmed-desorption of NH₃ was run from 40 to 800 °C at a heating rate of 10 °C/min. The desorbed ammonia was measured by a gas chromatograph (GC-SP6890, Shandong Lunan Ruihong Chemical Instrument Co. Ltd, Tengzhou China) with a thermal conductivity detector (TCD). Transmission Electron Microscopy (TEM) microphotographs were operated on JEOL-2010 electron microscope at 200 kV. The samples were suspended in ethanol. The loss of Co in the

reaction solutions was measured by Inductively Coupled Plasma Atomic Emission Spectroscopy (ICP-AES, Thermo-Jarrell ASH-Atom Scan Advantage). ICP-AES tests: after reaction, the reaction solution was centrifuged and evaporated to dryness under reduced pressure. The residue were dissolved with concentrated nitric acid and diluted with pure water. Scanning electron micrographs (SEM) of Co catalysts were taken using a scanning electron microscope (SEM, Sirion 200, FEI Electron Optics Company, USA).

$^1\text{H-NMR}$ and $^{13}\text{C-NMR}$ spectra were recorded on a Bruker Avance 400 spectrometer at ambient temperature. NMR spectra were analysed with MestReNova software.

Typical experiment and product analysis

If not stated otherwise, the reaction was carried out in an autoclave sponsored by Anhui Kemi Machinery Technology Co., Ltd. Usually, the initial temperature was $30\text{ }^\circ\text{C}$, then heating to the required reaction temperature through intelligent temperature controller in 0.5 h. After that the reaction was heating preservation with a certain period of time.

The typical experimental procedure was listed as follows:

The conversion of HMF was carried out in a 25 mL parr autoclave equipped with a magnetic stirrer, a temperature probe and a programmed temperature controller. The typical experiment was as follows: added 126 mg of substrate, 20 mg of catalyst, and 10 mL of methanol to the parr autoclave. Then tightened the screws and replaced the air with hydrogen four times. Filling hydrogen to the desired pressure at room temperature, Stirring and heating to the desired temperature under 500 rpm/min stirring. After maintaining the reaction for a certain period of time, decreased temperature and released pressure. The solution was transferred out with 20 mL of methanol, and a certain amount of N, N-dimethylformamide (DMF) was added as an internal standard. After centrifugation, the supernatant was analyzed by the Gas Chromatography (SHIMADZU, GC-2014C) equipped with the DM-Wax capillary column ($30\text{ m} \times 0.32\text{ mm} \times 0.25\text{ m}$). The conversion of HMF and the yield of products were calculated as follows:

$$\text{Conversion } \% = \frac{n_{\text{HMF}} - n'_{\text{HMF}}}{n_{\text{HMF}}} \times 100 \%$$

$$\text{Yield } \% = \frac{n_{(\text{mole of product})}}{n_{\text{HMF}}} \times 100 \%$$

n_{HMF} : mol of HMF before reaction

n'_{HMF} : mol of HMF after reaction

Results and Discussion

The effects of metallic metals and metal oxide catalysts on product distribution were examined initially; the results are summarized in Table 1.

Exploratory catalyst screening showed that metallic Fe catalyst did not catalyze the reaction compared with other metallic metals (Table 1, Entries 1–5). This might be because the metallic Fe catalyst is more susceptible to oxidation and

subsequent loss of activity. Selective conversion of HMF into BHMf was achieved by using both metallic Cu catalyst, Raney Ni, Raney Co catalysts (Table 1, Entries 1, 4 and 5). However, etherified products were not obtained. Metallic Co catalyst (Co-400) not only catalyzed the hydrogenation of HMF, but also promoted the etherification reaction, and mixtures containing significant amounts of hydrogenated and etherified product were obtained (Table 1, Entry 3). The unobserved formation of hydrolysis product methyl levulinate indicated that the catalyst had moderate Lewis acidity. Weaker Lewis acidity was observed according to $\text{NH}_3\text{-TPD}$ analysis (Figure S1). It is known that Brønsted acids and strong acid sites are more conducive to the production of alkyl levulinates, whereas the production of furanic ethers seems to be less demanding in terms of catalyst acidity.²⁶ Gorte *et al.* also reported that Sn-Beta catalyst, which only contains Lewis acid sites, was the most active catalyst for transfer hydrogenation of HMF and formation of etherified product.²⁷ The activity of several metal oxides was low, and no target products were obtained (Table 1, Entries 6–8). Lower conversion of HMF was obtained without catalyst, which confirmed that the catalyst had an important effect on product distribution (Table 1, Entry 9). Meanwhile, we found that the addition of acid (*eg.* H_2SO_4) had a weak inhibitory effect on the reaction, which might be due to an increased side reactions such as hydrolysis and oligomerization with an increased acidity (Table S1, Entry 1). The addition of base (*eg.* NaOH & Na_2CO_3) was not conducive to the production of BMMF, and the main product was hydrogenation product BHMf. The presence of bases inhibited the catalysis of Lewis acid, but did not inhibit the hydrogenation reaction (Table S1, Entry 1, Entry 2).

Table 1. Reductive etherification of HMF with different catalysts.^a

Entry	Catalyst	Conv. /%	Yield /%		
			BHMf	MMFA	BMMF
1	Metallic Cu	100.0	87.0	n.d	n.d
2	Metallic Fe	4.0	2.0	n.d	n.d
3	Co-400	100.0	8.4	28.4	62.3
4	Raney Ni	100.0	97.0	n.d	n.d
5	Raney Co	100.0	94.5	n.d	n.d
6	CuO^b	3.0	2.0	n.d	n.d
7	Fe_3O_4^b	1.0	n.d	n.d	n.d
8	Co_3O_4^b	3.0	n.d	n.d	n.d
9	-	1.0	n.d	n.d	n.d

[a] Reaction conditions: 126 mg HMF, 20 mg catalyst, 10 mL methanol, $120\text{ }^\circ\text{C}$, 1 h, 2 MPa H_2 , GC mole yield. [b] Commercial oxides were used directly without reduction. BHMf: 2,5-bis(hydroxymethyl)furan. MMFA: 5-methoxymethyl-furfuryl alcohol. BMMF: 2,5-bis(methoxymethyl)furan. n.d: not detected. Me: methyl.

To gain further insight into our reaction, we studied the reaction conditions in more detail.

Effect of reaction temperature

The reaction temperature had a significant effect on product distribution during the reaction, especially for the etherification process. We initially investigated the effect of different reaction temperatures on the product distribution (Figure 1). BHMF could be obtained almost quantitatively (93% yield) from HMF (94% conversion) at a lower temperature (90 °C). It was shown that the Co-400 catalyst had a high hydrogenation activity at lower temperature.²⁸ In our previous work, we also reported that the Co catalyst was more selective in hydrogenation of carbonyl groups.²⁵ At this point, no 5-methoxymethyl-furfuryl alcohol (MMFA) or 5-methoxymethyl-furfural (MFFA) was observed, which indicated that the catalytic system did not catalyze the etherification reaction of BHMF with methanol at lower temperature. It was reported that Co_3O_4 , which has Lewis acidity, did not catalyze the etherification at a lower temperature.²⁹ With the reaction temperature increased from 100 °C to 140 °C, HMF was completely converted and the yield of BHMF decreased gradually. Meanwhile, the yield of monoether MMFA increased initially, then decreased while the yield of BMMF gradually increased. The highest yield of BMMF was 98.5% at 140 °C and 1 h. This illustrated that the Co catalyst exhibited a certain acidity and promoted the rapid etherification reaction at higher temperature.

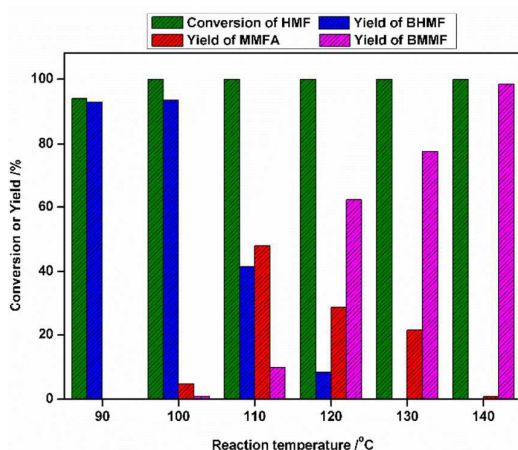


Figure 1. Reaction conditions: 126 mg HMF, 20 mg Co-400 catalyst, 10 mL methanol, 1 h, 2 MPa H_2 , GC mole yield.

It was found by XPS analysis that the Co^0 and $\text{Co}^{2+/3+}$ species coexist on the surface of catalyst, which indicated that the catalyst was only partially reduced during the reduction process (Figure 2a). According to XRD analysis, we found that only diffraction peaks arising from Co^0 species existed and no diffraction peaks associated with Co_3O_4 species were observed, indicating that Co_3O_4 was in an amorphous state in the Co catalyst (Figure 2b, 2c).³⁰ It was reported that more acidic sites existed in the amorphous state of Co_3O_4 than in the crystalline state, which facilitates the etherification reaction. The coexistence of Co^0 and $\text{Co}^{2+/3+}$ species on the surface of the catalyst was also more conducive to the electron transfer, which endows the catalyst with not only hydrogenation activity, but also with strong etherification activity.³¹

The preparation and characterization of Co catalysts with different reduction temperature were also carried out and investigated. The effect of catalytic reduction temperature on production distribution was carried out and the results were listed in Figure S2. Figure S3 were the XPS spectra of Co catalysts with different reduction temperature. And the surface composition of Co catalysts obtained from XPS analysis were listed in Table S5. The conversion of HMF and the yield of etherified products were too low by using Co-200 catalyst. Along with the increased reduction temperature, the yield of etherified products (MMFA, BMMF) increased initially and then decreased. From the Table S5, we found that the amount of Co^0 species were decreased and the amount of $\text{Co}^{2+}/\text{Co}^{3+}$ species were increased along with the increase of reduction temperature from 200 °C to 500 °C. The content of metal Co (Co^0) in the surface was lower after reduction at high temperature. This may be due to the reoxidation of highly active metal state Co species in the catalyst surface with higher reduction temperature. This indicated that the increase of substrate conversion and product yield was not just attributable to the proportion of Co^0 species on the surface. From Figure S4 of TEM images, the surface of Co catalyst turned porous after increase the reduction temperature from 200 °C to 300 °C (Figure S4a-b). Further increase the reduction temperature to 400 °C, the larger particles were formed due to the strong magnetism property of catalysts after reduction (Figure S4c). The particle size distribution of Co catalysts with different reduction temperature was calculated according to the TEM analysis and the results was listed in Figure S4d-e. It was found that the average particle size was 35 nm and 52 nm in Co-200 and Co-300 catalysts, respectively. This indicated that the particle size of Co catalyst was increased with the increase of reduction temperature. This was similar to the results observed in the TEM images. This was mainly due to the magnetic properties of the catalyst after reduction. The increase of reduction temperature led to the enhanced interaction of metal and ions, which could be also observed from the changed binding energy of Co^0 and $\text{Co}^{2+}/\text{Co}^{3+}$ species in XPS analysis (Figure S3). In order to better observe the morphology of the catalyst, we carried out the SEM analysis. It was found that the catalyst became more porous and rougher after reduction at high temperature (Figure S5a-c). This may be more beneficial for enhancing the selectivity of etherification product and the mass transfer of the reaction species.³²

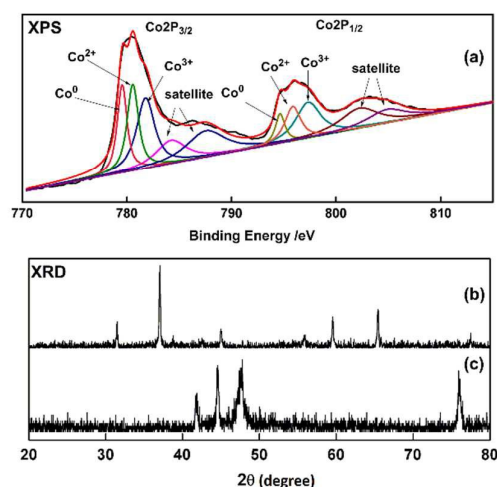


Figure 2. The XPS and XRD pattern of catalysts. (a) XPS pattern of Co-400 catalyst; (b) XRD pattern of Commercial Co_3O_4 . (c) XRD pattern of Co-400 catalyst.

Throughout the reaction process, we only observed the aldehyde hydrogenated product and etherified products rather than the products of over-hydrogenation of the furan ring (Figure 1). This result was presumably due to strong adsorption of the polar unsaturated aldehyde to the Co catalyst, whereas the unsaturated nonpolar double bonds on the furan rings are repelled. After the aldehyde group was adsorbed on the surface of the Co catalyst and hydrogenated to hydroxyl groups, the substrate would detach from the catalyst surface.³² It has been reported that H^+ ions ionized from H_2O or Lewis acid catalyst could promote the isomerization reaction of furfuryl alcohol or HMF.³³ However, we did not observe the formation of ring-opened products. In the reaction, no products of over-hydrolysis (e.g. levulinic acid and its esters) were observed, indicating that the Co-400 catalyst had high selectivity for reductive etherification.³⁴

The current catalytic system thus offers the significant advantage of allowing BMMF to be obtained by hydrogenation of HMF at low temperature ($90\text{ }^\circ\text{C}$), and BMMF to be obtained by etherification of BMMF at high temperature ($140\text{ }^\circ\text{C}$).

Effect of hydrogen pressure

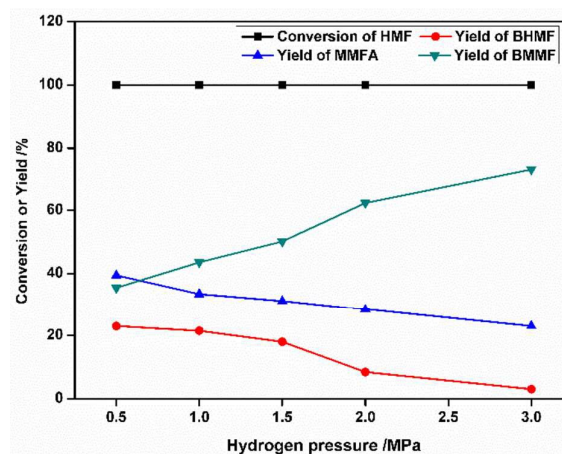


Figure 3. Reaction conditions: 126 mg HMF, 20 mg Co-400 catalyst, 10 mL methanol, 1 h, $120\text{ }^\circ\text{C}$, GC mole yield.

Then we investigated the effect of hydrogen pressure on product distribution (Figure 3). HMF could be completely converted at relatively low hydrogen pressure (0.5 MPa), and the main products were BMMF, MMFA, and BMMF. It was shown that the hydrogenation reaction and the etherification reaction could be carried out even at a relatively low pressure by using the Co-400 catalyst. With the hydrogen pressure increased from 1.0 MPa to 3.0 MPa, the yield of BMMF gradually decreased, the yield of monoether product MMFA decreased gradually, and the yield of diether product BMMF gradually increased. No significant change of carbon balance was observed, which indicated that the products were stable in the catalytic system under higher reaction pressure.

Effect of catalyst loading and substrate concentration

The effects of catalyst loading and substrate concentration on product distribution were investigated; the results are shown in Table 2. HMF could be completely converted and a mixture of products was obtained at 10 mg catalyst loading (Table 2, Entry 2). Increasing the amount of catalyst to 20 mg led to a significant decrease in the yield of BMMF and to a dramatic increase in the yield of BMMF (Table 2, Entry 1). Further increases in the amount of catalyst to 30 mg and 40 mg led to slight increases in the yield of etherified product (Table 2, Entries 3 and 4). This indicated that further increase in the amount of catalyst did not have a significant effect on product distribution. A suitable amount of catalyst was thus selected as 20 mg.

Then we studied the effect of substrate concentration on product distribution (Table 2, Entries 5–7). The data showed that the yield of etherified products gradually reduced while the yield of hydrogenated product BMMF gradually increased with an increase in the substrate concentration from 126 mg to 1000 mg. This was possibly caused by the two-step etherification reaction. Step one was the hydrogenation of HMF to BMMF, and the second step was etherification of BMMF to BMMF. An increase in the concentration of the substrate would allow more of the starting materials to be involved in the reaction than under the previous conditions (Table 2, Entry 1). If the

hydrogenation reaction was extended, and the time allowed for the subsequent etherified reaction was reduced accordingly, this would contribute to an increase in the amount of hydrogenation products. To verify this hypothesis, we extended the reaction time to 4 h and found that most of the BHMF was converted into a mixture of etherified products (Table 2, Entry 8). This further illustrated that a suitable substrate concentration was beneficial for achieving the desired product distribution.

Effect of reaction time

To understand the reaction mechanism involved in the reductive etherification of HMF to BMMF, we investigated the effect of reaction time on product distribution; the results are shown in Figure 4. The product distribution during the heating process was investigated initially. The reaction system was heated for 0.5 h from 30 °C to 120 °C, then the temperature was maintained for a defined period at 120 °C until the reaction reached completion. We investigated the effect of heating times on product distribution and the results were listed in Figure S6 (Heating times of 0.17 h, 0.34 h, and 0.5 h, respectively). HMF was not converted during the initial heating time of 0.17 h (internal temperature of ca. 60 °C), as shown in Figure S6. This indicated that the Co-400 catalyst did not catalyze the hydrogenation reaction at 60 °C. With the heating time extended to 0.33 h (internal temperature of ca. 90 °C), a small amount of HMF was converted and hydrogenated product of BHMF was obtained quantitatively. The hydrogenation activity of the catalyst was demonstrated at this temperature, but the hydrogenation activity remained weak. With the heating time extended to 0.5 h (internal temperature of ca. 120 °C), the conversion rate of HMF increased significantly (conversion of 36%), but only the hydrogenated product of BHMF was observed (yield of 35.7%). The reaction was then allowed to continue in the constant heating stage at 120 °C (Figure 4. "0 h" indicates the beginning of constant heating). We found that the Co-400 catalyst showed sufficient hydrogenation activity in the heating preservation stage. To study the distribution of reaction intermediates, we initially investigated the product distribution obtained from the constant heating stage of 0.17 h to 0.5 h.

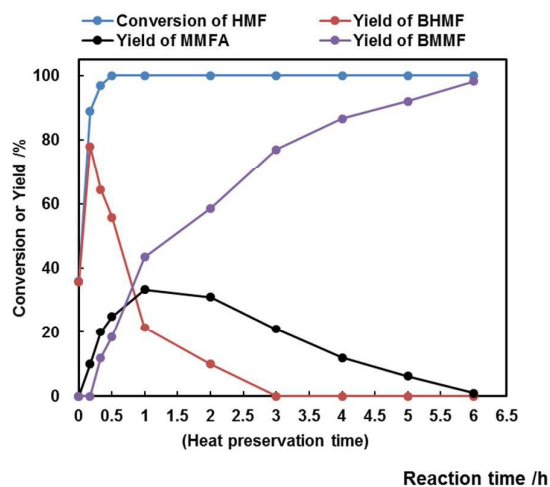


Figure 4. Reaction conditions: 126 mg HMF, 20 mg Co-400 catalyst, 10 mL methanol, 1 MPa H₂, 120 °C, GC mole yield.

In the constant heating time of 0.17 h, the conversion of HMF increased significantly (89%), which indicated the effective hydrogenation activity of the Co-400 catalyst on the aldehyde group. It also showed that the etherification reaction was more difficult than the hydrogenation reaction because no monoether product was observed at a constant heating time of 0.17 h. Meanwhile, the temperature had a significant influence on both the hydrogenation and etherification reactions. With a further extension of constant heating time to 0.33 h, the yield of BHMF

Table 2. Effect of catalyst amounts and substrate amounts on product distribution.^a

Entr y	catalyst amounts ^c	substrate amounts ^c	Conv./ %	Yield /%		
				BHMF	MMFA	BMMF
1	20	126	100.0	8.4	28.4	62.3
2	10	126	100.0	30.2	34.6	27.8
3	30	126	100.0	7.9	28.6	62.8
4	40	126	100.0	7.2	27.5	65.0
5	20	200	100.0	38.0	40.7	20.3
6	20	300	100.0	57.6	32.5	8.4
7	20	1000	100.0	84.1	14.3	0.5
8 ^b	20	1000	100.0	7.4	25.2	66.7

Reaction conditions: [a] 126 mg HMF, 20 mg Co-400 catalyst, 10 mL methanol, 120 °C, 1 h, 2 MPa H₂, GC mole yield. [b] 4 h. [c] The unit of catalyst amounts and substrate amounts is mg.

decreased as it was gradually converted into MMFA. BMMF was detected at a constant heating time of 0.33 h. At a constant heating time of 1 h, the yield of BHMF reduced to 21.5%, and a mixture of MMFA and BMMF ethers was found (yield of 33.4% and 43.5%, respectively). This showed that the degree of etherification gradually increased with extended reaction time at 120 °C. The yield of BMMF was obtained almost quantitatively (98.2%) when constant heating was extended to 6 h. We also found that 98.5% yield of BMMF could be obtained upon heating at 140 °C for 1 h as noted previously (Figure 1). This confirmed that the increased temperature could lead to a reduction in the etherification time and accelerate the reaction rate. Simultaneously, we found that no over-hydrolysis product methyl levulinate was observed in the reductive etherification reaction. This might be because the generated etherification products could inhibit the degradation reactions. After the etherification of intermediates, acid sites on the Co-400 catalyst may not catalyze the degradation reactions, thereby increasing the selectivity of the reaction. We also investigated the effect of reaction time on product distribution with high substrate concentration (1000 mg HMF/10 mL methanol) at 120 °C and 140 °C, respectively (Figure S7a, Figure 4). A similar product distribution was obtained at high substrate concentration (1000 mg HMF/10 mL methanol) compared to the reaction at low substrate concentration (126 mg HMF/10 mL methanol). However, the reaction time was extended along with the increased amount of substrate. The increase of temperature was advantageous for the conversion of HMF and the obtainment of ether products even at higher substrate concentration (Figure S7b).

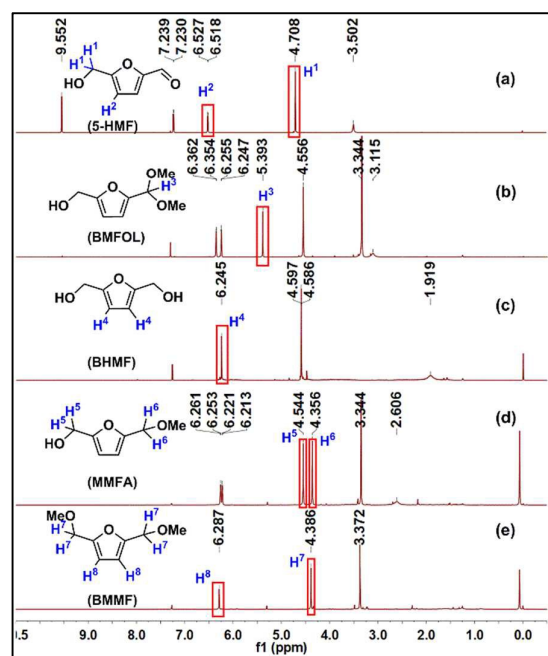


Figure 5. $^1\text{H-NMR}$ spectra of intermediates and products.

To analyze further the reaction process, the reaction solution with different reaction times (details of the treatment are given in the SI) was characterized by $^1\text{H-NMR}$ spectroscopic analysis. We initially assigned the characteristic peaks of $^1\text{H-NMR}$ for the possible intermediates in the reaction (Figure 5). The $^1\text{H-NMR}$ spectra of HMF, BMFOL, BHMF, MMFA, and BMMF, respectively, are shown in Figure 5a–e. The characteristic peaks of each material are indicated in red outlines. The characteristic peaks at ca. 4.71 ppm (Figure 5a, HMF, H^1) and ca. 6.51 ppm (Figure 5a, HMF, H^2) arise from hydrogen atoms on the furan ring and from the methylene of the hydroxymethyl group, respectively. The characteristic peaks at ca. 5.39 ppm (Figure 5b, BMFOL, H^3) arise from hydrogen atoms on the acetal. The characteristic peaks at ca. 6.24 ppm (Figure 5c, BHMF, H^4) originate from hydrogen atoms on the furan ring. The characteristic peaks at ca. 4.54 ppm (Figure 5d, MMFA, H^5) and ca. 4.36 ppm (Figure 5d, MMFA, H^6) arise from hydrogen atoms on the methylene of the hydroxymethyl group and from the methylene of the methoxy methyl group, respectively. The characteristic peaks at ca. 4.39 ppm (Figure 5e, BMMF, H^7) and ca. 6.29 ppm (Figure 5e, BMMF, H^8) arise from hydrogen atoms on the methylene of the methoxy methyl group and on the furan ring, respectively. Subsequently, $^1\text{H-NMR}$ analysis of the reaction solution with different reaction times was carried out; the results are presented in Figure 6. Likewise, we found that the product distribution obtained by $^1\text{H-NMR}$ analysis was similar to that of GC analysis. In the initial reaction process, only peaks arising from HMF were observed in the $^1\text{H-NMR}$ spectra (Figure 6a, ca. 6.51 ppm). With increased heating time, peaks arising from HMF decreased gradually and peaks from BHMF increased gradually according to the $^1\text{H-NMR}$ spectra (Figure 6b and Figure 6c, ca. 6.24 ppm). When the reaction was then submitted to constant heating (Figure 6d–k), peaks arising from

HMF disappeared after 0.33 h (Figure 6e). With prolonged constant heating, the intensity of the peaks arising from BHMF gradually decreased and disappeared at 3 h (Figure 6i). The intensity of peaks arising from MMFA increased first and then decreased (from Figure 6d to Figure 6k, ca. 4.54 ppm). The peaks arising from BMMF increased gradually with increased periods of constant heating and a nearly quantitative yield of BMMF was obtained at 6 h (Figure 6k, ca. 4.39 ppm).

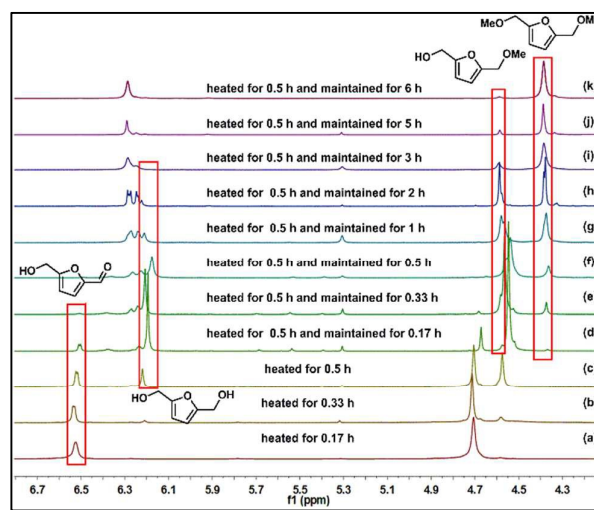


Figure 6. $^1\text{H-NMR}$ analysis of the reaction solution with different reaction times.

Catalyst recirculation

Given that the catalyst is magnetic, it could be adsorbed on a suitable magnet. Recycling experiments were therefore conducted as follows: after reaction, the magnet was taken out and washed with methanol three times before being put into the next cycle. The solution was transferred out with methanol and a defined amount of *N,N*-dimethylformamide (DMF) was added as an internal standard. After centrifugation, the supernatant was analyzed by gas chromatography. The catalyst adsorbed on the magnet was then put into the next cycle under the same reaction conditions. The experimental results obtained for catalyst recycling are summarized in Figure 7. The activity of the reused catalyst decreased slightly in terms of conversion and selectivity after five cycles. This was mainly due to the partial loss of catalyst during the posttreatment. We also investigated the leaching of metal Co in the reaction solution at 100 °C and 140 °C, respectively (Table S4). The leaching of metal Co were 0.2% and 0.7% at 100 °C (1h) and 140 °C (1h), respectively. This indicated that the leaching of Co in the reaction solution was very small during the reaction process. The use of alcohol solvent and partial neutral environment may be the reason for the less leaching of metal Co.

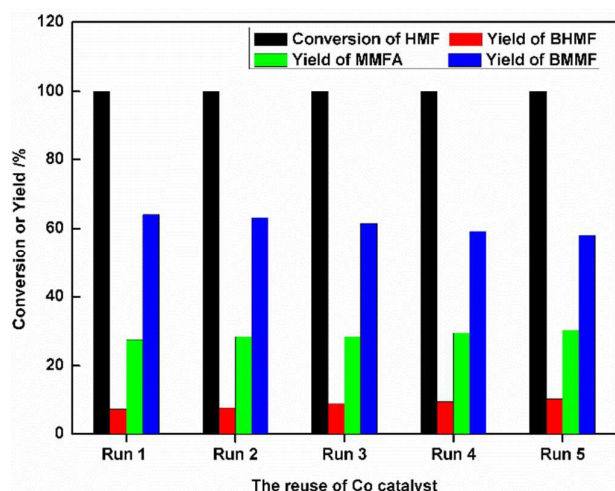


Figure 7. Reaction conditions: 126 mg HMF, 40 mg Co-400 catalyst, 10 mL methanol, 1 MPa H₂, 120 °C, GC mole yield.

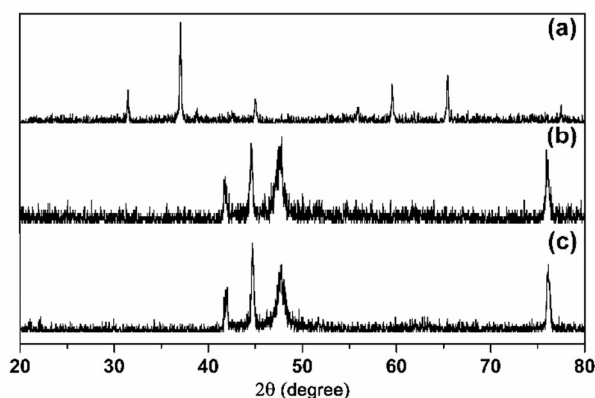


Figure 8. The XRD pattern of catalysts. (a) Commercial Co₃O₄. (b) Fresh Co-400 catalyst. (c) Co-400 catalyst after recycling five times.

Characterization by XRD and XPS analyses of both fresh and used catalysts was conducted (Figure 8 and Figure 9). No significant changes were found in the XRD pattern of the fresh and used catalysts. Compared with the fresh Co-400 catalyst, the proportion of Co⁰ species was decreased in the used catalyst according to the XPS analysis. The Co-400 catalyst had a better stability and could maintain a high reaction activity even after five times reuse in the methanol system.

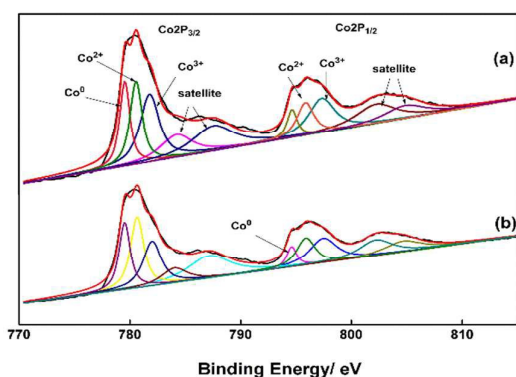
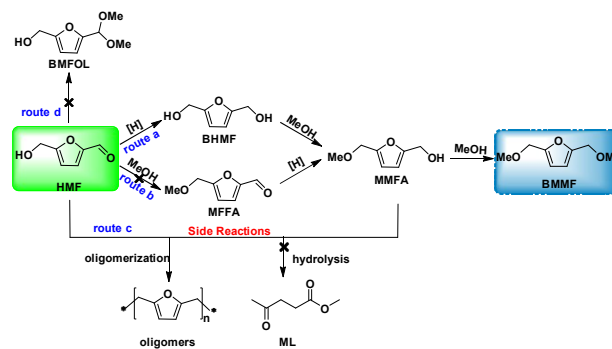
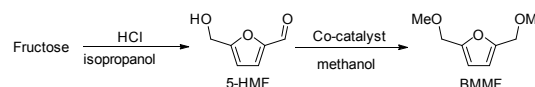


Figure 9. The XPS pattern of catalysts. (a) Fresh Co-400 catalyst. (b) Co-400 catalyst after recycling five times.



Scheme 2. Possible reaction pathways.

A possible pathway for the reductive etherification of HMF is shown in Scheme 2. Given that the Co-400 catalyst has both hydrogenation activity and etherification activity, the conversion of HMF might proceed in four ways: **route a**) the aldehyde group on HMF may be initially hydrogenated to obtain BHMFB in the presence of hydrogenation catalyst and hydrogen; **route b**) the hydroxyl group on HMF may be initially etherified to obtain MFFA by the catalyst³⁵; **route c**) HMF can be oligomerized to obtain oligomers or hydrolyzed to obtain methyl levulinate (ML) under catalysis³⁶; **route d**) aldolization of HMF and methanol to obtain BMFOL under catalysis.²⁰ Based on the experimental results and on characterization data, we have not found evidence for the presence of BMFOL, MFFA, and ML. Therefore, we suggest that **route a**) is the main reaction sequence. A possible reaction pathway is as follows. 1) The hydrogenation reaction of HMF to give BHMFB occurred on the hydrogenation sites of the Co-400 catalyst. Given the strong adsorption of C=O double bonds and the repellency of C=C double bonds of the metallic Co-400 catalyst, only the product BHMFB, arising from hydrogenation of the C=O double bonds, was obtained.³² 2) The etherification of BHMFB to give MMFA occurred followed by further etherification to obtain the target product BMMFB on the Lewis acid sites of the Co-400 catalyst. The reaction required a synergistic effect of hydrogenation activity and etherification activity. The coexistence of both Co⁰ and Co^{2+/3+} species on the surface of the Co-400 catalyst was more conducive to electron transfer and might be beneficial for high selectivity of the reaction. However, quantitative carbon yield was not obtained, perhaps because of oligomerization of HMF and intermediates (Scheme 2, **route c**). Further studies to establish the details of the mechanism are necessary.



Scheme 3. The preparation of BMMFB from fructose in two-steps.

Herein, we designed a two-steps method for the preparation of BMMFB from fructose (Scheme 3). Initial hydrolysis of fructose to HMF was achieved by using HCl catalyst and isopropanol

according to a reported procedure.³⁷ Reductive etherification of the obtained HMF by using the developed Co catalyst system was then undertaken to synthesize intermediate BMMF. The reaction was carried out in a 50 mL parr autoclave equipped with a magnetic stirrer, a temperature probe and a programmed temperature controller. 1 g of fructose, 10 μ L concentrated hydrochloric acid and 10 mL of isopropanol were added to parr autoclave. Stirring and heating to 120 $^{\circ}$ C under 500 rpm/min stirring and heat preservation at 120 $^{\circ}$ C for 2 h. Then removal of solvent under vacuum, and centrifugation after adding 3 mL water. The water layer was extracted three times with ethyl acetate, and the organic layer was dried with anhydrous sodium sulfate. Then removal of solvent under vacuum and 70% isolated yield of HMF was obtained. Subsequently the residue was diluted with 40 mL of methanol and transferred to the 50 mL parr autoclave. 80 mg of Co-400 catalyst was added and the reaction was carried out at 3 MPa H₂, 140 $^{\circ}$ C, 3 h. Conclusively filtrated the Co-400 catalyst and removed methanol, 95% yield of BMMF was obtained. The total isolated yield of BMMF was obtained as 66.5% from fructose.

Conclusions

The efficient reductive etherification of HMF to BMMF was carried out by using the simple reduced metallic Co catalyst. At 90 $^{\circ}$ C, 2 MPa H₂ and reaction time of 1 h, the yield of hydrogenated product BHMf was 93% and the conversion of HMF was 94% by using Co-400 catalyst. HMF was converted completely and 98.5% yield of etherified product BMMF was obtained at 140 $^{\circ}$ C, 2 MPa H₂, 1 h by using Co-400 catalyst. The coexistence of Co⁰ and Co^{2+/3+} species was observed on the surface of the Co catalyst according to XPS analysis. This might be more conducive to the electron transfer, which endows the catalyst not only with hydrogenation activity, but also with strong etherification activity. According to XRD analysis, we found that only the diffraction peaks arising from Co⁰ species were present, indicating that Co₃O₄ species were in an amorphous state in the Co catalyst. It was found that the catalyst had an appropriate acidity through NH₃-TPD characterization. The catalyst became more porous and rougher after reduction at high temperature according to the TEM and SEM analyses. This may be more beneficial for enhancing the selectivity of etherification product and the mass transfer of reaction species. The reaction processes were studied in detail by ¹H-NMR analysis and a possible reaction mechanism is proposed. A slight decrease in activity was attributed to the loss of catalyst during the cycle operations. Finally, 66.5% isolated yield of BMMF was obtained from fructose in two-steps.

Conflicts of interest

There are no conflicts to declare.

Acknowledgements

This work was supported by the NSFC (21572212, 21472033, and 21325208), MOST (2017YFA0303502), CAS (YZ201563), FRFCU and PCSIRT. The authors thank the Hefei Leaf Biotech Co., Ltd. and Anhui Kemi Machinery Technology Co., Ltd. for free samples and equipment that benefited our ability to conduct this study.

References

- (a) A. Corma, O. de la Torre, M. Renz, N. Villandier, *Angew. Chem. Int. Ed.*, 2011, **50**, 2375 – 2378; (b) Y. Nakagawa, S. B. Liu, M. Tamura, K. Tomishige, *ChemSusChem*, 2015, **8**, 1114 – 1132; (c) M. Stöcker, *Angew. Chem. Int. Ed.*, 2008, **47**, 9200 – 9211; (d) J. C. Serrano-Ruiz, R. M. West, J. A. Dumesic, *Annu. Rev. Chem. Biomol.*, 2010, **1**, 79 – 100; (e) H. Olcay, A. V. Subrahmanyam, R. Xing, J. Lajoie, J. A. Dumesic, G. W. Huber, *Energ. Environ. Sci.*, 2013, **6**, 205 – 216; (f) A. Corma, S. Iborra, A. Velty, *Chem. Rev.*, 2007, **107**, 2411 – 2502; (g) M. J. Gilkey, B. J. Xu, *ACS Catal.*, 2016, **6**, 1420 – 1436; (h) P. Gallezot, *Chem. Soc. Rev.*, 2012, **41**, 1538 – 1558; (i) M. Besson, P. Gallezot, C. Pinel, *Chem. Rev.*, 2014, **114**, 1827 – 1870; (j) D. M. Alonso, S. G. Wettstein, J. A. Dumesic, *Chem. Soc. Rev.*, 2012, **41**, 8075 – 8098.
- (a) H. Li, S. Saravanamurugan, S. Yang, A. Riisager, *Green Chem.*, 2016, **18**, 726 – 734; (b) G. A. Kraus, T. Guney, *Green Chem.*, 2012, **14**, 1593 – 1596.
- (a) G. S. Yi, S. P. Teong, Y. G. Zhang, *Green Chem.*, 2016, **18**, 979 – 983; (b) G. S. Yi, S. P. Teong, X. K. Li, Y. G. Zhang, *ChemSusChem*, 2014, **7**, 2131 – 2137; (c) G. S. Yi, S. P. Teong, Y. G. Zhang, *ChemSusChem*, 2015, **8**, 1151 – 1155; (d) J. P. Ma, Z. T. Du, J. Xu, Q. H. Chu, Y. Pang, *ChemSusChem*, 2011, **4**, 51 – 54; (e) H. L. Wang, Y. X. Yang, T. S. Deng, C. M. Chen, Y. L. Zhu, X. L. Hou, *ACS Catal.*, 2015, **5**, 5636 – 5646; (f) X. X. Liu, H. Ding, Q. Xu, W. Z. Zhong, D. L. Yin, S. P. Su, *J. Energ. Chem.*, 2016, **25**, 117 – 121.
- (a) X. Tang, J. N. Wei, N. Ding, Y. Sun, X. H. Zeng, L. Hu, S. J. Liu, T. Z. Lei, L. Lin, *Renew. Sust. Energ. Rev.*, 2017, **77**, 287 – 296; (b) M. J. Climent, A. Corma, S. Iborra, *Green Chem.*, 2014, **16**, 516 – 547; (c) N. Perret, A. Grigoropoulos, M. Zanella, D. T. Manning, J. B. Claridge, M. J. Rosseinsky, *ChemSusChem*, 2016, **9**, 521 – 531.
- (a) T. Komanoya, T. Kinemura, Y. Kita, K. Kamata, M. Hara, *J. Am. Chem. Soc.*, 2017, **139**, 11493 – 11499; (b) A. Dunbabin, F. Subrizi, J. M. Ward, T. D. Sheppard, H. C. Hailes, *Green Chem.*, 2017, **19**, 397 – 404; (c) S. Sowmiah, L. F. Veiros, J. M. S. S. Esperanca, L. P. N. Rebelo, C. A. M. Afonso, *Org. Lett.*, 2015, **17**, 5244 – 5247; (d) Q. Girka, N. Hausser, B. Estrine, N. Hoffmann, J. L. Bras, S. Marinković, J. Muzart, *Green Chem.*, 2017, **19**, 4074 – 4079.
- (a) J. Ohyama, R. Kanao, A. Esaki, A. Satsuma, *Chem. Commun.*, 2014, **50**, 5633 – 5636; (b) J. Ohyama, R. Kanao, Y. Ohira, A. Satsuma, *Green Chem.*, 2016, **18**, 676 – 680; (c) M. H. Zhou, Z. Zeng, H. Y. Zhu, G. M. Xiao, R. Xiao, *J. Energy. Chem.*, 2014, **23**, 91 – 96.
- (a) G. W. Huber, J. N. Chheda, C. J. Barrett, J. A. Dumesic, *Science*, 2005, **308**, 1446 – 1450; (b) D. J. Liu, E. Y. X. Chen, *ChemSusChem*, 2013, **6**, 2236 – 2239; (c) A. Corma, O. D. L. Torre, M. Renz, N. Villandier, *Angew. Chem. Int. Ed.*, 2011, **50**, 2375 – 2378; (d) A. D. Sutton, F. D. Waldie, R. Wu, M. Schlaf, L. A. P. Silks, III, J. C. Gordon, *Nat. Chem.*, 2013, **5**, 428 – 432.
- (a) L. Hu, L. Lin, Z. Wu, S. Y. Zhou, S. J. Liu, *Renew. Sust. Energ. Rev.*, 2017, **74**, 230 – 257; (b) R. J. van Putten, J. C. van der Waal, E. de Jong, C. B. Rasrendra, H. J. Heeres, J. G. de Vries, *Chem. Rev.*, 2013, **113**, 1499 – 1597; (c) Y. Nakagawa, M. Tamura, K. Tomishige, *ACS Catal.*, 2013, **3**, 2655 – 2668; (d)

- J. H. Dai, L. F. Zhu, D. Y. Tang, X. Fu, J. Q. Tang, X. W. Guo, C. W. Hu, *Green Chem.*, 2017, **19**, 1932 – 1939.
- 9 C. C. Chang, S. K. Green, C. L. Williams, P. J. Dauenhauer, W. Fan, *Green Chem.*, 2014, **16**, 585.
- 10 (a) K. S. Arias, M. J. Climent, A. Corma, S. Iborra, *ChemSusChem*, 2014, **7**, 210 – 220; (b) M. Mascal, E. B. Nikitin, *Green Chem.*, 2010, **12**, 370 – 373; (c) M. Mascal, E. B. Nikitin, *Angew. Chem., Int. Ed.*, 2008, **47**, 7924 – 7926; (d) M. Mascal, E. B. Nikitin, *ChemSusChem*, 2009, **2**, 423 – 426.
- 11 E. de Jong, T. Vijlbrief, R. Hijkoop, G.-J. M. Gruter, J. C. van der Waal, *Biomass Bioenerg.*, 2012, **36**, 151 – 159.
- 12 (a) M. Paniagua, J. A. Melero, J. Iglesias, G. Morales, B. Hernández, C. L. Aguado, *Appl. Catal. A-Gen.*, 2017, **537**, 74 – 82; (b) J. D. S. Smith, L. Baldwin, A. Chafin, P. A. Goodman, *ChemistryOpen*, 2016, **5**, 297 – 300.
- 13 (a) G. A. Kraus, T. Guney, *Green Chem.*, 2012, **14**, 1593 – 1596; (b) C. M. Lew, N. Rajabbeigi, M. Tsapatsis, *Ind. Eng. Chem. Res.*, 2012, **51**, 1538 – 5366; (c) S. Alipour, H. Omidvarborna, D. S. Kim, *Renew. Sust. Energ. Rev.*, 2017, **71**, 908 – 926; (d) J. M. Wang, Z. H. Zhang, S. W. Jin, X. Z. Shen, *Fuel*, 2017, **192**, 102 – 107; (e) S. S. Yin, J. Sun, B. Liu, Z. H. Zhang, *J. Mater. Chem. A.*, 2015, **3**, 4992 – 4999; (f) H. Li, S. Saravanamurugan, S. Yang, A. Riisager, *Green Chem.*, 2016, **18**, 726 – 734; (g) G. A. Kraus, T. Guney, *Green Chem.*, 2012, **14**, 1593 – 1596; (h) H. L. Wang, Y. X. Wang, T. S. Deng, C. M. Chen, Y. L. Zhu, X. L. Hou, *Catal. Commun.*, 2015, **59**, 127 – 130.
- 14 (a) J. E. Zanetti, *J. Am. Chem. Soc.*, 1927, **49**, 1065 – 1067; (b) G. Morales, M. Paniagua, J. A. Melero, J. Iglesias, *Catal. Today*, 2017, **279**, 305 – 316.
- 15 K. Iwanami, K. Yano, T. Oriyama, *Chem. Lett.*, 2007, **36**, 38 – 39.
- 16 (a) K. C. Nicolaou, C.-K. Hwang, D. A. Nugiel, *J. Am. Chem. Soc.*, 1989, **111**, 4136 – 4137; (b) M. Bakos, Á. Gyömöre, A. Domján, T. Soós, *Angew. Chem., Int. Ed.*, 2017, **56**, 5217 – 5221.
- 17 M. P. Doyle, D. J. DeBruyn, D. A. Kooistra, *J. Am. Chem. Soc.*, 1972, **94**, 3659 – 3661.
- 18 M. B. Sassaman, G. K. Surya Prakash, G. A. Olah, *Tetrahedron*, 1988, **44**, 3771 – 3780.
- 19 C. F. Zhao, C. A. Sojda, W. Myint, D. Seidel, *J. Am. Chem. Soc.*, 2017, **139**, 10224 – 10227.
- 20 M. Balakrishnan, E. R. Sacia, A. T. Bell, *Green Chem.*, 2012, **14**, 1626 – 1634.
- 21 G. J. M. Gruter, *US8231693B2*, 2012.
- 22 Q. Cao, W. Y. Liang, J. Guan, L. Wang, Q. Qu, X. Z. Zhang, X. C. Wang, X. D. Mu, *Appl. Catal. A-Gen.*, 2014, **481**, 49 – 53.
- 23 (a) H. Li, Z. Fang, R. L. S. Jr, S. Yang, *Prog. Energ. Combust.*, 2016, **55**, 98 – 194; (b) J. Jae, E. Mahmoud, R. F. Lobo, D. G. Vlachos, *ChemCatChem*, 2014, **6**, 508 – 513; (c) J. D. Lewis, S. V. de Vyver, A. J. Crisci, W. R. Gunther, V. K. Michaelis, R. G. Griffin, Y. R. Leshkov, *ChemSusChem*, 2014, **7**, 2255 – 2265.
- 24 (a) Z. Y. Wu, P. Chen, Q. S. Wu, L. F. Yang, Z. Pan, Q. Wang, *Nano Energy*, 2014, **8**, 118 – 125; (b) Z. Z. Wei, J. Wang, S. J. Mao, D. F. Su, H. Y. Jin, Y. H. Wang, F. Xu, H. R. Li, Y. Wang, *ACS Catal.*, 2015, **5**, 4783 – 4789.
- 25 X. L. Li, J. Deng, J. Shi, T. Pan, C. G. Yu, H. J. Xu, Y. Fu, *Green Chem.*, 2015, **17**, 1038 – 1046.
- 26 P. Neves, M. M. Antunes, P. A. Russo, J. P. Abrantes, S. Lima, A. Fernandes, M. Pillinger, S. M. Rocha, M. F. Ribeiro, A. A. Valente, *Green Chem.*, 2013, **15**, 3367 – 3376.
- 27 J. Luo, J. Y. Yu, R. J. Gorte, E. Mahmoud, D. G. Vlachos, M. A. Smith, *Catal. Sci. Technol.*, 2014, **4**, 3074 – 3081.
- 28 G. H. Wang, X. Deng, D. Gu, K. Chen, H. Tüysüz, B. Spliethoff, H. J. Bongard, C. Weidenthaler, W. Schmidt, F. Schüth, *Angew. Chem., Int. Ed.*, 2016, **55**, 11101 – 11105.
- 29 H. Wu, G. Pantaleo, G. D. Carlo, S. Guo, G. Marci, P. Concepción, A. M. Venezia, L. F. Liotta, *Catal. Sci. Technol.*, 2015, **5**, 1888 – 1901.
- 30 W. Q. Qin, C. R. Yang, X. H. Ma, S. S. Lai, *J. Alloys Compd.*, 2011, **509**, 338 – 342.
- 31 X. D. Yan, L. H. Tian, M. He, X. B. Chen, *Nano Lett.*, 2015, **15**, 6015.
- 32 H. C. Zhou, J. L. Song, H. L. Fan, B. B. Zhang, Y. Y. Yang, J. Y. Hu, Q. G. Zhu, B. X. Han, *Green Chem.*, 2014, **16**, 3870 – 3875.
- 33 (a) Y. L. Yang, Z. T. Du, Y. Z. Huang, F. Lu, F. Wang, J. Gao, J. Xu, *Green Chem.*, 2013, **15**, 1932 – 1940; (b) M. Hronec, K. Fulajtarová, *Catal. Commun.*, 2012, **24**, 100; (c) M. H. Zhou, Z. Zeng, H. Y. Zhu, G. M. Xiao, R. Xiao, *J. Energ. Chem.*, 2014, **23**, 91 – 96.
- 34 Q. Cao, J. Guan, G. M. Peng, T. G. Hou, J. W. Zhou, X. D. Mu, *Catal. Commun.*, 2015, **58**, 76 – 79.
- 35 Z. H. Wang, Q. W. Chen, *Green Chem.*, 2016, **18**, 5884 – 5889.
- 36 S. K. R. Patil, C. R. F. Lund, *Energy Fuels*, 2011, **25**, 4745 – 4755.
- 37 L. K. Lai, Y. G. Zhang, *ChemSusChem*, 2011, **4**, 1745 – 1748.